ELSEVIER

Journal of Photochemistry and Photobiology A: Chemistry 110 (1997) 59–65

Journal of PHOTOCHEMISTRY AND PHOTOBIOLOGY A: CHEMISTRY

Re-absorption and excitation energy transfer of *N,N'*-bis(2,5-di-tert-butylphenyl)-3,4:9,10-perylenebis(dicarboximide) (DBPI) laser dye

Samy A. El-Daly [a,*], Satoshi Hirayama [b]

[a] *Chemistry Department, Faculty of Science, Tanta University, Tanta, Egypt*

[b] *Kyoto Institute of Technology, Matsugasaki, Sakyo, Kyoto 606, Japan*

Received 2 January 1997; revised 8 April 1997; accepted 21 April 1997

Abstract

The effect of re-absorption on the excited state lifetime and emission spectrum of *N,N'*-bis(2,5-di-tert-butylphenyl)-3,4:9,10-perylenebis(dicarboximide) (DBPI) was investigated in chloroform. Increasing the concentration of DBPI above 5×10^{-5} M causes a significant change in the fluorescence spectral shape and an increase in the excited state lifetime.

Excitation energy transfer from DBPI to malachite green (MG) was also studied in different solvents by measuring the fluorescence decay and steady state emission. The rate constants of energy transfer k_{ET} were determined to be 8.4×10^{10}, 7.7×10^{10} and 3.9×10^{11} M^{-1} s^{-1} in methanol, butanol and ethylene glycol respectively. The experimental critical transfer distances were calculated to be 52.5 Å in methanol, 50.2 Å in butanol and 53.9 Å in ethylene glycol. The activation energies E_a for fluorescence quenching of DBPI by MG and KI were calculated to be 4.5 and 9.22 kJ mol^{-1} respectively. © 1997 Published by Elsevier Science S.A.

Keywords: *N,N'*-Bis(2,5-di-tert-butylphenyl)-3,4:9,10-perylenebis(dicarboximide); Excitation energy transfer; Re-absorption

1. Introduction

The dyes derived from 3,4:9,10-perylenetetracarboxylic dianhydride have been known for several decades as vat dyes possessing excellent light fastness [1–3], but only recently has it been recognized that the photochemical stability of the dyes is retained in solution phase and that the fluorescence quantum yields are high [4–6]. These properties make perylene dyes attractive as potential laser dyes [7,8], photosensitizers for electron transfer reactions [9–11] and as solar concentrators [12]. Perylene derivatives have also been found to include some promising microcrystalline photoconductors for electrophotography [13], and have been incorporated in prototype solar photovoltaic cells [14].

In previous papers, certain characteristics of *N,N'*-bis(2,5-di-tert-butylphenyl)-3,4:9,10-perylenebis(dicarboximide) (DBPI) have been investigated, e.g. the laser activity, effect of the medium polarity and acidity on the electronic absorption and emission spectra, energy transfer from blue laser dyes [7] and deactivation of the excited singlet state by cobalt ions and molecular oxygen [15,16].

In this paper, the effect of the concentration on the excited state lifetime and emission spectrum of DBPI was studied, together with the deactivation of the excited singlet state by malachite green (MG) and potassium iodide (KI) in different media.

2. Experimental details

DBPI (Aldrich) was dissolved in a minimum volume of chloroform; the dye was precipitated by adding methanol. The precipitate was collected by filtration and dried in vacuum. MG was of guaranteed grade (Wako Pure Chem. Ind.). All the solvents used in this work were of spectroscopic grade.

The fluorescence decay curves were measured in a conventional 1 cm cuvette, monitoring the emission at right angles using time-correlated single-photon counting (TCSPC). The decay curves were analysed using the method of iterative, non-linear, least squares [17]. The experimental details of the fluorescence decay curve measurements and the analysis of the decay data have been described elsewhere [18]. The sample solutions were deaerated with either solvent-saturated argon or nitrogen gas for 20 min.

Steady state emission spectra were measured with a Shimadzu RF 510 spectrofluorophotometer connected to an ultrathermostat (Julabo F 10; temperature precision, ±0.1 °C) using a rectangular quartz cell of dimensions 0.2 cm × 1

* Corresponding author.

PII S1010-6030(97)00132-9

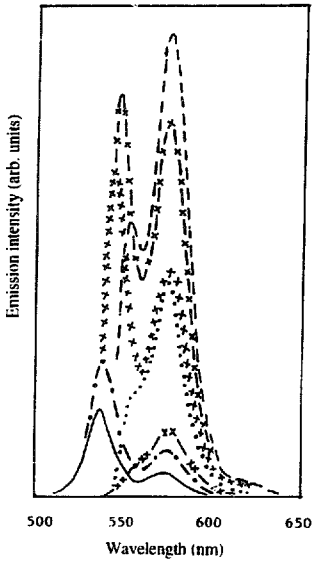

Fig. 1. Emission spectra (λ_{ex} = 420 nm) of 1×10^{-6} (——), 5×10^{-6} (– · –), 1×10^{-5} (× × ×), 5×10^{-5} (– × –), 1×10^{-4} (····· ——), 8×10^{-4} (· · ·) and 1×10^{-3} (– × × –) mol dm^{-3} DBPI in $CHCl_3$.

cm to minimize re-absorption. The emission was monitored at right angles. UV–visible absorption spectra were measured using a Shimadzu UV-2100S spectrophotometer.

The room temperature fluorescence quantum yields $\phi_f(s)$ were calculated relative to the fluorescence quantum yield of rhodamine 6G (R6G) as a reference standard, for which $\phi_f = 0.96$ in ethylene glycol [19], using the relation

$$\phi_f(s) = \phi_f(r)\frac{\int I_s(\bar{\nu})\,d\bar{\nu}}{\int I_r(\bar{\nu})\,d\bar{\nu}} \times \frac{A_r}{A_s} \times \frac{n_s^2}{n_r^2} \qquad (1)$$

The indices s and r denote the sample and reference respectively. The integrals represent the corrected fluorescence peak areas; A and n are the absorbance at the excitation wavelength and the refractive index of the applied solvent respectively.

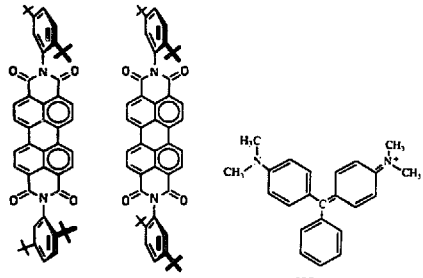

3. Results and discussion

3.1. Effect of concentration

Fig. 1 shows the emission spectra (λ_{ex} = 420 nm) of DBPI in chloroform recorded at different concentrations. The emission intensity decreases with increasing concentration in the range 1×10^{-4} to 1×10^{-3} mol dm^{-3}. This decrease in the emission intensity of DBPI is due to the strong overlap between the emission and absorption spectra of DBPI in chloroform, as shown in Fig. 2, leading to re-absorption of the emitted photons by ground state DBPI molecules. The overlap integral (J), which expresses the degree of spectral overlap between the emission and absorption spectra, was calculated using Eq. (2) [20] as $J = 13.4\times10^{-13}$ M^{-1} cm^3

$$J = \int_0^{\infty} \frac{F(\bar{\nu})\epsilon(\bar{\nu})}{(\bar{\nu})^4}\,d\bar{\nu} \qquad (2)$$

where $F(\bar{\nu})$ is the emission intensity normalized to unity and $\epsilon(\bar{\nu})$ is the molar absorptivity of DBPI.

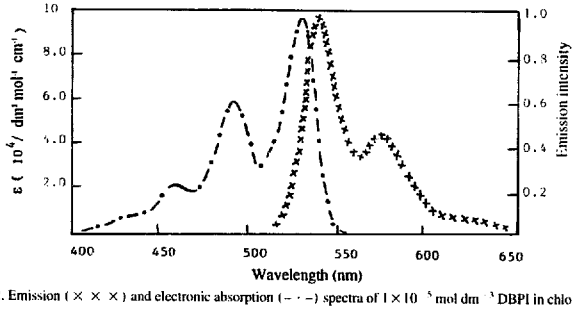

Fig. 2. Emission (× × ×) and electronic absorption (– · –) spectra of 1×10^{-5} mol dm^{-3} DBPI in chloroform.

Table 1
Fluorescence lifetime (τ), probability of re-absorption (a) and the average number of re-absorption cycles $\langle n \rangle$ at different concentrations of DBPI in $CHCl_3$ ($\lambda_{ex} = 420$ nm, $\lambda_{em} = 530$ nm)

[DBPI] (mol dm^{-3})	τ (ns)	$\langle n \rangle$	a	ϕ_f
1×10^{-6}	3.70	1.000	0.0	0.98
5×10^{-6}	3.71	1.005	0.005	
1×10^{-5}	3.98	1.075	0.07	
5×10^{-5}	5.09	1.375	0.275	
1×10^{-4}	5.52	1.491	0.272	
5×10^{-4}	7.42	2.001	0.505	
1×10^{-3}	8.52	2.230	0.556	

The electronic absorption spectrum of DBPI in chloroform does not change with concentration, indicating the absence of molecular aggregation of DBPI in this solvent.

Re-absorption was confirmed by measuring the fluorescence lifetime at different concentrations of DBPI in chloroform. As shown in Table 1, the fluorescence lifetime increases with concentration from 3.7 ns at 1×10^{-6} mol dm^{-3} to 8.52 ns at 1×10^{-3} mol dm^{-3}. However, the decay curves remain single exponential over the whole concentration range examined, indicating the absence of excimer emission.

The apparent fluorescence lifetime τ can be related to the true fluorescence lifetime τ_M by the average number of re-absorption cycles $\langle n \rangle$ [17,18] such that

$$\tau = \langle n \rangle \tau_M \tag{3}$$

For values of $\langle n \rangle$ smaller than 1.1, Scully et al. [21] observed a single exponential fluorescence decay of R6G, but above this value a convex decay profile with a rising component of R6G was obtained. For DBPI, however, the fluorescence decay remains single exponential even at $\langle n \rangle = 2.23$ as shown in Fig. 3. The probability of re-absorption a was calculated from Eq. (4) [17]

$$\tau = \frac{\tau_M}{1 - a q_{FM}} \tag{4}$$

where τ_M is the molecular fluorescence lifetime (i.e. as measured at infinite dilution), τ is the apparent fluorescence lifetime, a is the probability of self-re-absorption (which depends on the overlap between the emission and absorption spectra as well as the path length of fluorescence through the sample) and q_{FM} is the molecular quantum yield. Table 1 summarizes the fluorescence lifetime, the probability of re-absorption and the number of re-absorption cycles at each concentration of DBPI dye.

3.2. Fluorescence quenching of DBPI by MG

Excitation energy transfer from DBPI to MG was studied in different solvents, such as methanol, butanol and ethylene glycol, by steady state emission and lifetime measurements.

The electronic absorption spectrum of DBPI shows no changes when MG is added, indicating the absence of ground state complex formation between DBPI and MG. From the emission spectra of DBPI measured in the absence and presence of MG, there is no evidence of exciplex formation between excited DBPI and MG dye. As shown in Fig. 4, a decrease in emission intensity is observed on addition of MG to DBPI without discernible changes in the maximum or shape of the fluorescence spectrum accompanied by quenching.

The apparent second-order rate constant k_{ET} for energy transfer in the DBPI–MG pair can be calculated from the Stern–Volmer plots shown in Fig. 5 which obey Eq. (5)

$$\frac{I_0}{I} = 1 + k_{ET}\tau_f[MG] \tag{5}$$

where I_0 and I represent the fluorescence intensities of DBPI in the absence and presence of MG; I was corrected for the inner filter effect using the equation given in Ref. [22]; τ_f is the solution lifetime of the donor in the absence of the acceptor. From the slopes of the Stern–Volmer plots and the solution lifetime of DBPI, the values of k_{ET} were calculated to be 8.6×10^{10}, 8.1×10^{10} and 3.7×10^{11} M^{-1} s^{-1} in methanol, butanol and ethylene glycol respectively.

From the fluorescence lifetime measurements, k_{ET} can be calculated using Eq. (6) [23]

$$k_{ET}[MG] = \frac{1}{\tau_f} - \frac{1}{\tau_0} \tag{6}$$

where τ_f and τ_0 are the calculated best-fit exponential decay times for DBPI in the presence and absence of MG respectively. As shown in Fig. 6, the observed fluorescence decay curve can approximately be fitted to a single exponential

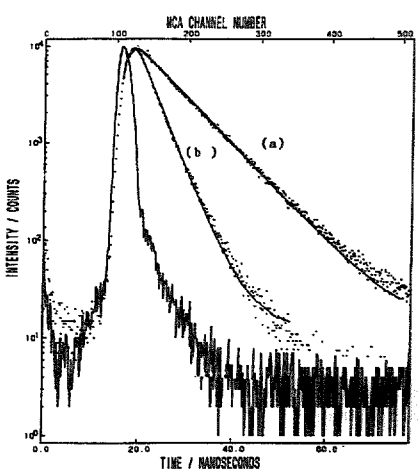

Fig. 3. Fluorescence decay curves of (a) 5×10^{-6} and (b) 1×10^{-3} mol dm^{-3} DBPI in chloroform.

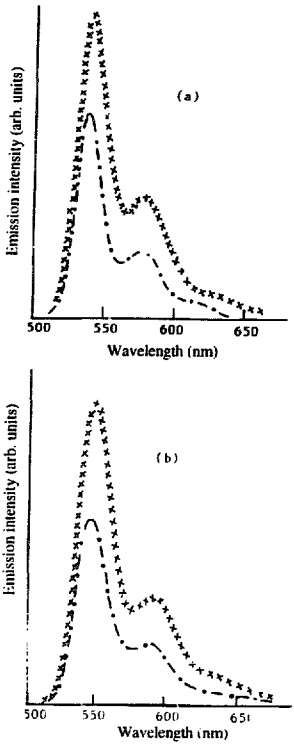

Fig. 4. (a) Emission spectra of 5×10^{-6} mol dm^{-3} DBPI in the absence (× × ×) and presence (– · –) of 2×10^{-4} mol dm^{-3} MG in methanol (λ_{ex}=420 nm). (b) Emission spectra of 5×10^{-6} mol dm^{-3} DBPI in the absence (× × ×) and presence (– · –) of 4×10^{-4} mol dm^{-3} MG in ethylene glycol (λ_{ex}=420 nm).

function. Therefore Eq. (6) is used instead of the more accurate equation of the $t^{1/2}$ function [24] in order to obtain approximate values for k_{ET}. The k_{ET} values are 8.4×10^{10}, 7.72×10^{10} and 3.9×10^{11} M^{-1} s^{-1} in methanol, butanol and ethylene glycol respectively, which are in good agreement with those obtained from the steady state emission measurements, indicating the absence of static quenching. As shown in Table 2, the rate of energy transfer k_{ET} is larger than the diffusion rate constant k_{diff} for all solvents used in this work, and the value of k_{ET} in ethylene glycol is much greater than those in methanol and butanol, indicating that translation diffusion is not a governing factor in the quenching mechanism of the DBPI–MG pair [25].

Since there is good overlap between the emission spectrum of DBPI and the absorption spectrum of MG, as shown in Fig. 7, a long-range energy transfer mechanism is expected. The critical transfer distance R_0 at which 50% of the excitation energy is transferred to the acceptor can be calculated using the Förster formula [26]

$$R_0^6=\frac{1.25\times10^{-25}\times\phi_f}{n^4}\int_0^\infty\frac{F_D(\bar{\nu})\epsilon_A(\bar{\nu})}{(\bar{\nu})^4}d\bar{\nu} \quad (7)$$

where ϕ_f is the emission quantum yield of the donor in the absence of the acceptor, n is the solvent refractive index, $F_D(\bar{\nu})$ is the normalized distribution of the donor emission at wavenumber $\bar{\nu}$ (cm^{-1}) and $\epsilon(\bar{\nu})$ is the decadic molar absorption coefficient of the acceptor.

The R_0 values are 52.5, 50.1 and 53.9 Å in methanol, butanol and ethylene glycol respectively, and comparable with those obtained for the resonance energy transfer studies of other donor–acceptor pairs using different techniques [26]. The large values of the critical transfer distance and the rate constant of energy transfer indicate that the underlying mechanism for the DBPI–MG pair is resonance energy transfer due to long-range dipole–dipole interaction between the excited donor and the ground state acceptor.

The effect of temperature on the energy transfer from excited DBPI to MG was also studied in methanol in the temperature range 15–45 °C. The values of the activation energy E_a associated with k_{ET} were calculated by assuming the Arrhenius equation for k_{ET}

$$k_{ET}=A\exp(-E_a/RT) \quad (8)$$

The value obtained for E_a is 4.5 kJ mol^{-1}, which is much smaller than the E_a value of about 10–13 kJ mol^{-1} expected for diffusion-controlled quenching in methanol.

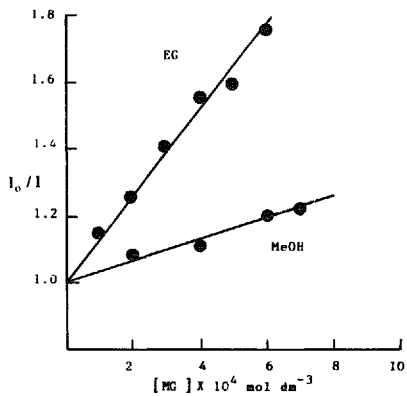

Fig. 5. Stern–Volmer plots of the fluorescence quenching of 5×10^{-6} mol dm^{-3} DBPI by MG in methanol (MeOH) and ethylene glycol (EG) (λ_{ex}=420 nm, λ_{em}=530 nm).

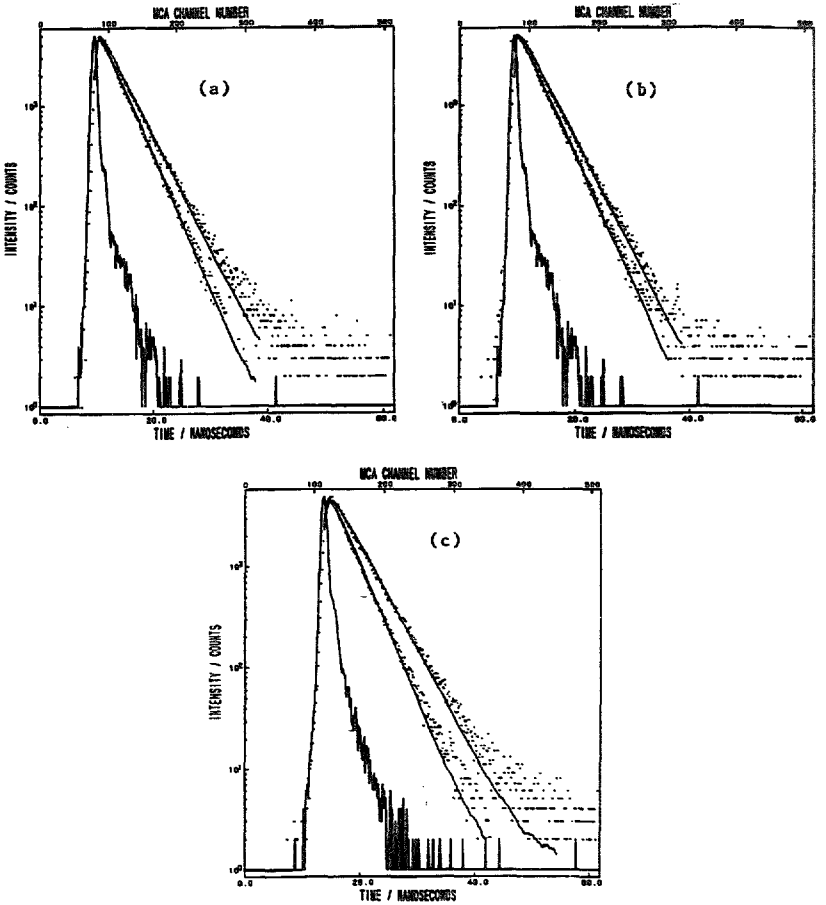

Fig. 6. Fluorescence decay curves of 5×10^{-6} mol dm^{-3} DBPI in the absence and presence of MG (λ_{ex} = 420 nm) in methanol ([MG] = 5×10^{-4} mol dm^{-3}) (a), butanol ([MG] = 5.2×10^{-4} mol dm^{-3}) (b) and ethylene glycol ([MG] = 1.25×10^{-4} mol dm^{-3}) (c).

Table 2
Rate constants of energy transfer for DBPI–MG pair in different solvents

Solvent	[MG] (mol dm^{-3})	τ_0 (ns)	τ (ns)	$k_{ET}/10^{10}$ (M^{-1} s^{-1})	$k_{diff}/10^{10}$ (M^{-1} s^{-1})
MeOH	5×10^{-4}	3.79	3.27	8.4 [a] (8.67) [b]	1.8
Butanol	5.2×10^{-4}	3.79	3.29	7.7 [a] (8.1) [b]	0.34
Ethylene glycol	1.25×10^{-4}	3.76	3.18	39 [a] (37) [b]	0.057

τ is the lifetime of DBPI in the presence of MG.
τ_0 is the lifetime of DBPI in the absence of MG.
[a] Calculated from lifetime measurements.
[b] Calculated from steady state emission measurements.

Table 3
Fluorescence lifetimes of DBPI in the absence (τ_0) and presence (τ) of KI and quenching rate constants (k_q) in different solvents ([DBPI] = 5×10^{-6} mol dm^{-3}, [KI] = 0.012 mol dm^{-3}, λ_{ex} = 420 nm, λ_{em} = 530 nm)

Solvent	ϕ_f	τ_0 (ns)	τ (ns)	$k_q/10^{10}$ ($M^{-1}s^{-1}$)	$k_{diff}/10^{10}$ ($M^{-1}s^{-1}$)
MeOH	0.98	3.70	2.65	1.04	1.8
EtOH	0.97	3.59	3.03	0.43	0.92
1-Propanol	0.95	3.58	3.27	0.223	0.54
2-Propanol	0.95	3.54	3.33	0.15	0.35

Table 4
Effect of temperature on the fluorescence quenching rate constant of DBPI by KI in MeOH

T (°C)	$k_q/10^{10}$ ($M^{-1}s^{-1}$)
20	1.04
25	1.30
30	1.37
35	1.46
40	1.55
45	1.62

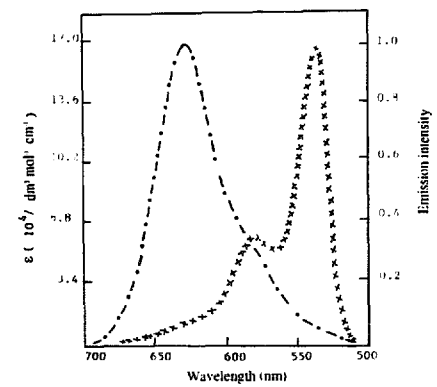

Fig. 7. Emission spectrum (× × ×) of 5×10^{-6} mol dm^{-3} DBPI (λ_{ex} = 420 nm) and electronic absorption spectrum (– · · –) of 1×10^{-5} mol dm^{-3} DBPI in ethylene glycol.

3.3. Fluorescence quenching by KI

The fluorescence quenching of DBPI by KI was also studied in different polar solvents using steady state emission and lifetime measurements. Iodide ions quench the fluorescence by enhancing intersystem crossing via a spin–orbit coupling mechanism [27,28]; the bimolecular quenching rate constants k_q were calculated using the Stern–Volmer plots and Eq. (6).

As can be seen from Table 3, the bimolecular quenching rate constant k_q decreases with increasing medium viscosity; the k_q values are close to the diffusion-controlled bimolecular reaction rate constant k_{diff}, given by $8RT/2000\eta$, indicating a collisional quenching mechanism for the DBPI–I system.

The effect of temperature on the fluorescence quenching was also studied in methanol, as shown in Table 4. The k_q values increase with increasing temperature.

The activation energy E_a associated with k_q in methanol was calculated to be 9.2 ± 0.5 kJ mol^{-1}. This value is very close to the activation energy associated with the solvent viscosity (E_η = 10.4 kJ mol^{-1} in methanol) [14], though this does not necessarily indicate that the fluorescence quenching of DBPI by KI is fully diffusion controlled, as has been extensively discussed for various anthracene derivative–O_2 systems [29,30].

4. Conclusions

The emission intensity and excited state lifetime of DBPI in chloroform are strongly affected by the concentration. Increasing the concentration of DBPI causes a significant change in the fluorescence spectral shape and an increase in the excited state lifetime.

The electronic energy transfer from DBPI to MG obeys a Förster-type mechanism in the form of a long-range dipole–dipole interaction between excited donor and ground state acceptor, whereas the fluorescence quenching of DBPI by iodide ions obeys a spin–orbit coupling mechanism.

References

[1] T. Maki, H. Hashimato, Bull. Chem. Soc. Jpn. 25 (1952) 411.
[2] T. Maki, H. Hashimato, Bull. Chem. Soc. Jpn. 27 (1954) 602.
[3] K. Venkataraman, The Chemistry of Synthetic Dyes, Vol. 2, Academic Press, New York, 1952, pp. 1188–1194.
[4] H. Langhals, Chem. Ber. 118 (1985) 4641.
[5] W.E. Ford, J. Photochem. 34 (1986) 43.
[6] W.E. Ford, P.V. Kamat, J. Phys. Chem. 91 (1987) 6373.
[7] E.M. Ebeid, H. Langhals, S.A. El-Daly, J. Phys. Chem. 92 (1988) 4565.
[8] M. Sadrai, L. Hadel, R. Sauer, S. Husain, K. Jespersen, J.D. Westbrook, G.R. Bird, J. Phys. Chem. 96 (1992) 7988.
[9] V. Balzan, F. Bolleta, F. Scandola, R. Ballardini, Pure Appl. Chem. 51 (1979) 299.
[10] J.R. Darwent, P. Douglas, A. Harriman, G. Porter, M.C. Richoux, Coord. Chem. Rev. 44 (1982) 83.
[11] G.J. Kavarnos, N.J. Turro, Chem. Rev. 86 (1986) 401.
[12] M. Sandrai, G.R. Bird, Opt. Commun. 51 (1984) 62.
[13] Z.D. Popovic, R.O. Loutfy, A.M. Hor, Can. J. Chem. 63 (1985) 134.
[14] P. Panayotatos, D. Parikh, R.R. Sauers, G.R. Bird, A. Piechowski, S. Husain, Solar Cells 18 (1986) 71.

[15] S.A. El-Daly, J. Photochem. Photobiol. A: Chem. 68 (1992) 51.
[16] S.A. El-Daly, M. Okamoto, S. Hirayama, J. Photochem. Photobiol. A: Chem. 91 (1995) 105.
[17] J.B. Birks, Photophysics of Aromatic Molecules, Wiley-Interscience, New York, 1970, p. 92.
[18] Y. Sakai, M. Kawahigashi, T. Minami, T. Inoue, S. Hirayama, J. Lumin. 42 (1989) 317.
[19] A. Harriman, J. Chem. Soc., Faraday Trans. 1 76 (1980) 1978.
[20] J.R. Lakowicz, Principles of Fluorescence Spectroscopy, Plenum, New York, 1983, p. 306.
[21] A.D. Scully, A. Matsumoto, S. Hirayama, J. Lumin. 157 (1991) 253.
[22] B. Marciniak, J. Chem. Educ. 63 (1986) 998.
[23] A.D. Scully, T. Takeda, M. Okamoto, S. Hirayama, Chem. Phys. Lett. 228 (1994) 32.
[24] K.K. Pandey, S. Hirayama, J. Photochem. Photobiol. A: Chem. 99 (1996) 165.
[25] A.S. Azim, M.A. El-Kemary, S.A. El-Daly, H.A. El-Daly, M.E. El-Khouly, E.M. Ebeid, J. Chem. Soc., Faraday Trans. 2 92 (1996) 747.
[26] S.A. El-Daly, S.A. Azim, H.A. El-Daly, K. Abou-Zeid, J. Chim. Phys. 92 (1995) 1195.
[27] A.R. Watkins, J. Phys. Chem. 78 (1974) 2555.
[28] D.O. Cowan, R.L.E. Drisko, J. Am. Chem. Soc. 92 (1970) 6281.
[29] S. Hirayama, H. Yasuda, A.D. Scully, M. Okamoto, J. Phys. Chem. 98 (1994) 4609.
[30] K.K. Pandey, M. Okamoto, S. Hirayama, Chem. Phys. Lett. 224 (1994) 417.